

SUPPLEMENTARY MATERIAL, Guo *et al.*

SUPPLEMENTAL METHODS:

Reagents and cell culture: All reagents were of analytical grade from Sigma (St. Louis, MO) unless otherwise stated. Cell culture media and reagents were from Gibco (Grand Island, NY). Cell culture plastics were from Corning (Corning NY). Gases were from Airgas Inc. (Radnor, PA). Consumables for the XF-24 were from Seahorse Bioscience (Billerica, MA). The Spectrum Collection™ chemical library was from Microsource Discovery Inc. (Gaylordsville, CT), supplied through the University of Rochester high throughput screening core. The complete list of molecules in the library is available at <http://www.msdiscovery.com>. The library was stored at -80°C on 96-well plates at 1 mM in DMSO.

Initial experiments (not shown) were attempted with isolated adult rat cardiomyocytes, but the high degree of variability between preparations results in inconsistent levels of cell death in the screen. In addition, a primary reason for developing this screen was to avoid the use of large numbers of animals to determine cardioprotective efficacy. The use of primary cells (1 rat = cells for 1 plate, thus 39 plates = 39 rats) would compromise this ethical goal. Thus a cell line was chosen for subsequent analysis. The rat cardiomyocyte derived H9c2 cell line was obtained from ATCC (Manassas, VA) at passage 13, and maintained at sub-confluence in DMEM with 25 mM glucose, 1 mM pyruvate, 4 mM glutamine, 10% FBS and pen/strep, at 37°C with 5% CO₂. Cells were used between passages 20 and 40, plated on XF-24 V7-PET plates at 15-30,000 cells/well, 24-48 hrs. prior to testing. One hr. prior to assay, media was replaced with 700 µl assay media (DMEM with 25 mM glucose, 1 mM pyruvate, 4 mM glutamine, no serum, no antibiotics, no bicarbonate, pH 7.4 at 37°C).

Physical adaptation of the XF-24 instrument and consumables: The Seahorse XF-24 measures O₂ consumption rate (OCR) and extracellular acidification rate (ECAR) by intact cells, in 24-well plate format¹. Atop the cell culture plate sits a disposable spring-loaded cartridge, with 24 plungers which travel in a vertical axis controlled by the instrument. Embedded in the

plunger tips are fluorescent porphyrin probes sensitive to pO_2 and pH, which are interrogated by fiber-optics. Lowering the plungers creates a transient 7 μ l micro-chamber in each well, allowing OCR and ECAR measurements. Raising the probes re-exposes cells to the bulk media, allowing repeat measurements, and/or drug delivery via injection ports located alongside the plungers (see schematic, main manuscript Fig. 1).

Holding down the plungers, cells will eventually consume the available O_2 in the transient 7 μ l micro-chamber, simulating an ischemic state. Raising the plungers simulates reperfusion by flooding the cells with bulk media. While cellular respiration alone could be used to bring down the pO_2 within the micro-chamber, molecules that impact mitochondrial function may affect the degree of ischemia attainable. Thus, the XF24 was adapted for delivery of argon gas in the head-space of the measurement cartridge, to provide additional control over O_2 levels.

Gas flow was delivered to the cartridge head space by Luer (ISO 594) fittings. This was achieved by drilling 4 holes (one per corner) in the disposable XF cartridge, using a water-cooled 4.2mm bit. As shown in Online Figure I A, a Tygon tube was fed via the ventilation panel in the rear of the instrument, through into the read chamber, along the route of the fiber-optic bundle to the read head. There, as shown in Fig. Online Figure I B, the tube was split into 2, then 4 silicon tubes, each of which delivered gas to a corner of the plate. These wider diameter tubes were chosen for their ease of breakage away from the Luer connectors, to avoid damage to the instrument mechanical systems in case of an unscheduled operation such as cartridge ejection.

The insulating aluminum side-plates attached to the read head were machined for cut-outs to permit the rear gas delivery holes to be placed on the sides of the cartridge. This was done to avoid interference with the screw which controls the height of the read head, which is located immediately behind the cartridge. The front holes were drilled in the front of the cartridge, with the right-side hole being drilled as far to the right as possible (next to the plate indentation), to avoid collision with the plate-grabbing solenoid. In this configuration, the cartridge and read-head were permitted their normal range of motion, and all machine operations requiring movement of the read head (mix, delay, measure, inject, etc.) could be achieved without disturbance.

The XF instrument contains two sensors which detect the removal of the main cover. One of these, a mechanical switch on the left of the chamber, was locked in the closed position using electrical tape. The second is a light-sensor located on the right, close to the sample loading door. Temporary positioning of a razor blade in front of this sensor (Online Figure I C) ensured the instrument did not abort the protocol due to the cover being removed. Following replacement of the main cover, removal of the blade was essential to permit normal operation (plate loading etc.)

Gas flowing into the headspace of the plate was controlled from outside the instrument as follows: a tank of argon gas was connected to a regulator, then to a humidifier (10 ml. tube with frit, filled with 3 ml. deionized water), a flow meter, and finally to the tube in the rear of the XF instrument. For reperfusion purposes, room air was pumped into the same system via a small electric pump. Humidification of incoming gases was essential, to prevent evaporation of the sample due to heating inside the instrument.

Changes to assay work-flow: The typical work-flow of an XF experiment is as follows:

- (i) Plate cells. Hydrate cartridge overnight.
- (ii) Transfer cells to assay media and place in incubation side of instrument sample tray (37 °C). Load test compounds into cartridge.
- (iii) Load cartridge and calibrate it.
- (iv) Eject calibration plate. Transfer cell plate across to read position, begin protocol.
- (v) At end of protocol, eject cartridge and cell plate together.

For the purposes of this ischemia-reperfusion model, the assay workflow was adjusted, to allow fitting of gas delivery tubes during the pre-calibration phase. The following protocol was used (changes underlined):

- (i) Plate cells. Drill holes in cartridge and hydrate it overnight.
- (ii) Transfer cells to assay media and place in incubation side of instrument sample tray (37 °C). Load test compounds into cartridge.

- (iii) Load cartridge. During 20 min. pre-calibration wait (instrument status reads “waiting after lowering cartridge), remove cover* and fit gas lines to cartridge. Close cover, and proceed with calibration.
- (iv) Eject calibration plate. Transfer cell plate across to read position, begin read protocol.
- (v) At end of protocol, do not eject. Remove cover* and remove all tubing, then replace cover before proceeding with eject function.

*Temporary Placement of razor blade to disable light sensor.

Removal of the main instrument cover, fitting gas lines, and replacement of the cover, could be accomplished within ~40 s. Performing this operation at the beginning of the 20 min. wait period before calibration ensured maximal remaining time for the interior of the instrument to re-gain temperature stability prior to calibration. Use of the thermal block (a machined metal block mounted on the sample tray) was essential to provide additional thermal mass and stability.

XF Instrument Protocol: The protocol in the XF software was as follows:

- (i) Calibrate. Equilibrate.
- (ii) 2 cycles [Mix 1 min., Wait 2 min., Measure 2 min.]
- (iii) Inject all 4 ports (A, B, C, D) containing test molecules and vehicle controls.
- (iv) Mix 1 min., Wait 2 min., Measure 2 min.
- (v) Begin argon flow, at 500ml/min.
- (vi) 5 cycles [Mix 10 s., Wait 5 min., Mix 10 s., Measure 30s.]
- (vii) Measure 60 min (this is the nominal “ischemia” period, with plungers down).
- (viii) Stop argon flow, flush with room air.
- (ix) Mix 5 min., Wait 2 min., Stop room air flow, Measure 2 Min.
- (x) Wait 60 min.
- (xi) 2 cycles [Mix 1 min., Wait 2 min., Measure 2 min.]

Steps (ii) and (iv) served to obtain pre- and post-injection measurements of ECAR and OCR, to assess the metabolic effects of injected molecules. The protocol in step (vi) was determined empirically to afford the maximum rate of deoxygenation of the media. Due to the design of the instrument, the “Mix” cycle changes the volume of the head-space between the cartridge and plate. Thus, keeping mix times short ensured that argon was not flushed out from the head space during mixing. Short read times during this period were required only to monitor the pO₂ of the bulk media, not for obtaining OCR values (typically OCR requires a longer read time, to obtain sufficient values at 12 s. per cycle, for a slope fit).

Step (vii) was the actual ischemia phase, during which cells were trapped in the transient 7 µl micro-chamber. Step (xi) served to obtain post-IR measurements of ECAR and OCR, to gauge recovery of these parameters by comparison with pre-IR values (step (iv)).

IR injury protocol and end-points: Typical traces of pO₂ and pH throughout the IR protocol, averaged from 22 wells on a plate (20 molecule test wells and vehicle 2 controls), are shown in the main manuscript Fig. 2. Pre-ischemic measurements of OCR and ECAR were obtained both prior to and after injection of test molecules. Flow of humidified argon was then initiated at 500 ml/min., followed 35 min. later by lowering of the plungers for 60 min., during which time cells bought the pO₂ in the transient micro-chamber to 0.37 ±0.01 mmHg, modeling ischemia. pH was also monitored throughout, and fell by approximately 1 unit while plungers were lowered. After 1 hr., argon flow to the cartridge was replaced with room air, plungers were raised, and the bulk media mixed for 5 min., representing reperfusion. Measurements of OCR and ECAR were obtained immediately post-reperfusion, and again 1 hr. later.

The “LEVEL (CURVE FIT)” algorithm within the XF-24 software was used to calculate pO₂. Notably, while another commonly used algorithm (“AKOS”) is recommended for measurements at low O₂ levels, this algorithm corrects for O₂ diffusion through the plastic of the cell plate, and in doing so assumes the instrument is filled with room air. Owing to the use of argon to flood the plate in this system, the AKOS algorithm could not be used.

Cell Death Assay: Following the IR protocol, cell death was assayed by the luminometric Cytotox-Glo™ assay (Promega, Madison WI) according to the manufacturer's protocol, on a Spectramax™ plate reader (Molecular Devices, Sunnyvale CA).

Correction for plate position bias: Despite randomization of test molecules and controls on each plate, a small degree of bias was observed wherein certain wells consistently exhibited a higher or lower cell death than normal (if all wells were equal then average cell death in each well across all 39 plates should be 1.0). This deviance from the norm was attributed to edge effects in cell culture² or variations in conditions inside the instrument such as temperature or gas flow. If uncorrected, such factors could generate false positives or negatives in the assay, e.g., assignment of protection to a test molecule when in-fact part of its protective score was due to being in a well that always exhibits protection, regardless of what is added.

To correct for this phenomenon, the mean cell death in each well across all 39 plates was mapped (Online Figure IV). The map shows that indeed some wells exhibited higher or lower scores than normal. Individual cell death values on each plate were then corrected using the map, as outlined in the following example (reminder, scores <1 = protective, scores >1 = detrimental):

- (i) Plate 6, well B6, original cell death score = 0.88
- (ii) Average cell death in well B6 across all 39 plates = 0.82
- (iii) "Map-corrected" cell death in well B6 = $(0.88-1)-(0.82-1)+1 = 1.06$

Thus, well B6 on this plate gave a mild protective score, but well B6 was biased toward protective scores in general, so correcting for this bias canceled the protective score, yielding a slightly detrimental score. Of 550 wells in Round 1 (500 test wells, 50 controls), 22 false hits were reassigned as non-hits, with 18 wells vice versa. Of 308 wells in round 2 (224 test compounds, 84 controls), 30 false hits were reassigned as non-hits, with 5 wells vice versa. Altogether, 8.70% of wells were re-assigned by the application of the map. The method was better at removing false hits than assigning hit status to initially non-hit wells. All data in

Supplementary Table I and main manuscript Figures 3, 4, & 6 are presented as map-corrected scores.

First round screen: Test molecules were diluted to 20 μ M in assay media on the day of the experiment, and 70 μ l loaded into cartridge injection ports (Fig. 1), for a final injected concentration of 1.43 μ M (DMSO 0.57 % vol). A multiplex strategy was used, with 4 molecules per well in each of 20 test wells on the XF plate (80 molecules per plate x 25 plates = 2000 molecules). Two wells were used for background correction (media alone) and two for vehicle controls (no test molecules).

It was originally intended to normalize cell death in the molecule test wells to the 2 control wells on each plate. However, this was not possible due to excessive noise between the control wells (i.e. if one control well was an outlier, it could lead to a biased assignment of test molecules as either protective or detrimental, relative to controls). Therefore, cell death in each well was instead expressed relative to the mean for the whole plate, including both controls and test wells. This normalization requires that the molecule library is a random distribution of protective/inactive/detrimental molecules, a fact supported by Online Figure III A.

An alternative approach would be to use more control wells on each plate, but this would decrease the number of available wells for test molecules. The plating of the library master stock (80 molecules per plate on 96-well layout) was conveniently matched to the 96-well layout of the injection ports on the XF cartridge, to permit rapid loading of molecules each day. Therefore, adding more controls and disrupting this loading pattern would not only increase the total number of plates required, but would drastically slow both upstream sample handling and downstream data analysis.

Second round screen: 56 wells (224 molecules) exhibiting the lowest post-IR cell death scores in round 1 were split up and their components tested at 1-molecule-per-well. Each plate comprised 16 molecule test wells, 2 background correction wells, and 6 vehicle controls (14 plates x 16 molecules = 224). This sub-set of the library was assumed biased toward protective molecules, which would preclude normalization of cell death to the plate average (as in round 1).

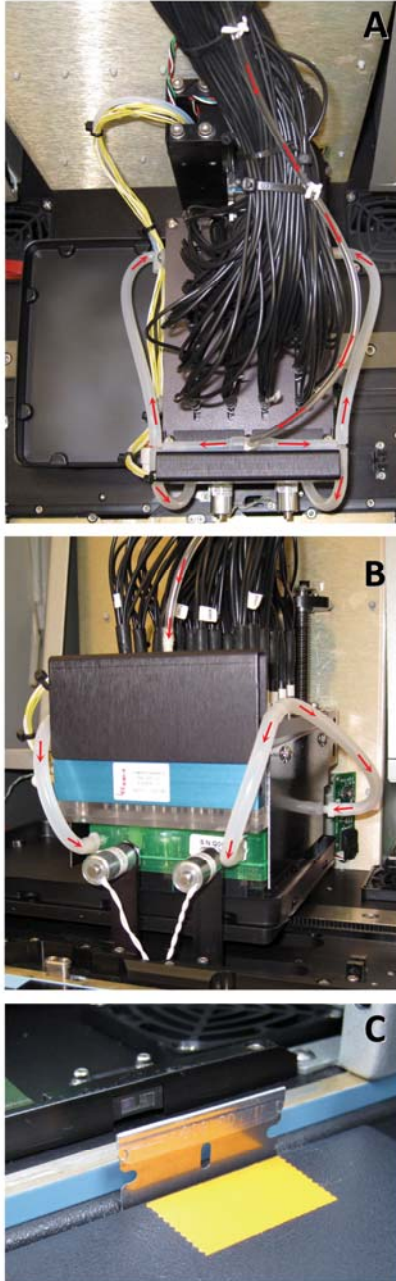
Therefore, cell death in round 2 was expressed relative to the 6 vehicle controls on each plate. This greater number of controls abrogated the noise issues experienced in round 1.

Development of hits: Male Sprague-Dawley rats, 200-250 grams, were obtained from Harlan (Indianapolis IN) and maintained in accordance with the NIH *Guide for the Care and Use of Laboratory Animals*. A Langendorff perfused heart model of IR injury was employed, as previously described³ In brief, hearts were perfused with Krebs Henseleit buffer in constant flow mode (12 ml/min.), with left ventricular pressure monitored by a balloon and transducer linked to a digital collection device (Dataq, Akron OH). Hearts were subjected to 35 min. global ischemia and 2 hrs. reperfusion, followed by assessment of infarct size by tetrazolium chloride staining⁴. Six test compounds were administered at 1 μ M for 20 min. prior to ischemia, via a syringe port directly above the perfusion cannula. Importantly, independent groups of control hearts (IR alone) were used for each test molecule.

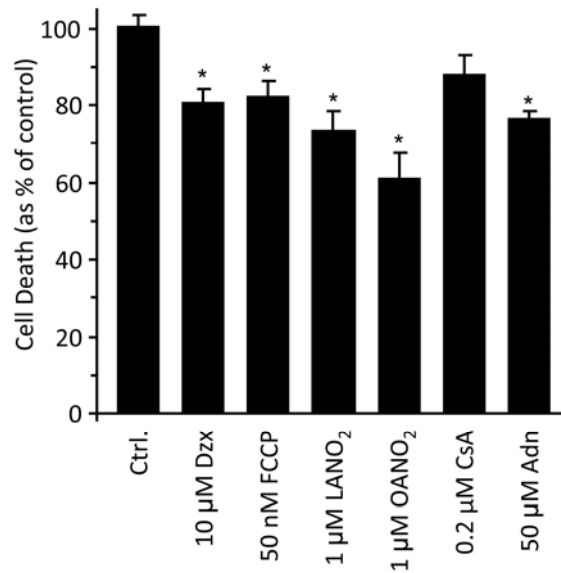
Statistical methods and correlations: For comparisons between groups, unless otherwise indicated, multi-way ANOVA was used, with significance (p) set at 0.05. For correlations (main manuscript Fig. 5) linear regression curve fit was used. r^2 was calculated using the “RSQ” function of Microsoft Excel™ software. The significance of correlations was calculated using equation [1]...

$$t = \frac{\sqrt{r^2}}{\sqrt{1-r^2}/DF} \quad [1]$$

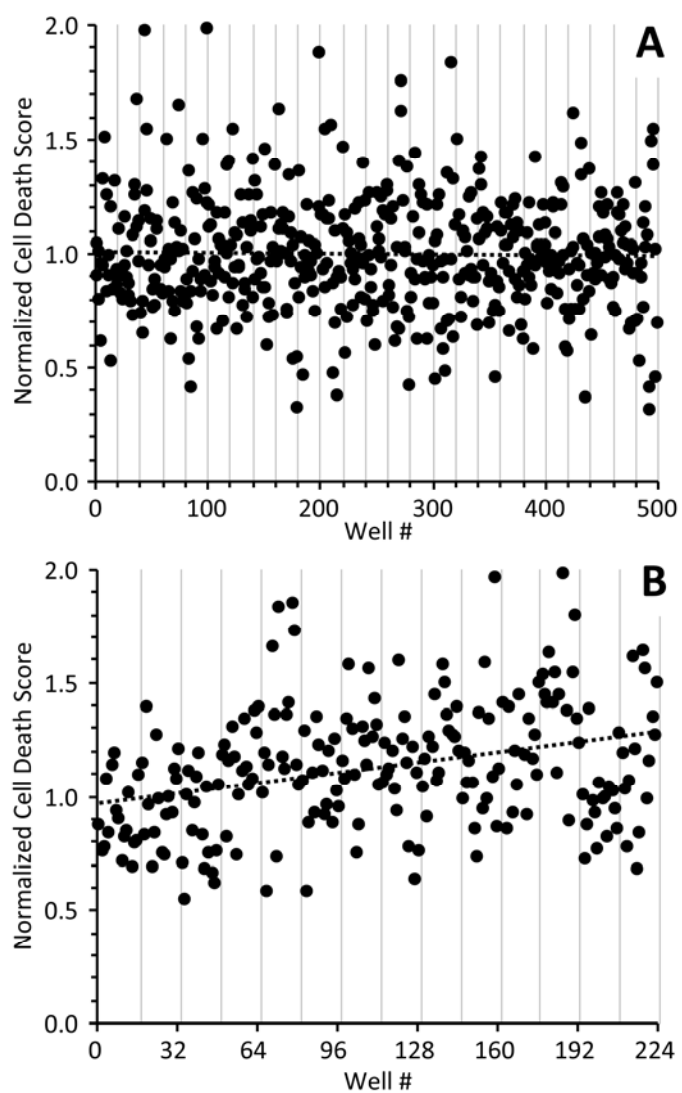
...in which DF is degrees of freedom (N-2). Significance (p) was calculated from t using the TDIST function of Microsoft Excel™, with a p value <0.05 considered significant. A Bonferroni correction was applied to correct for multiple regression analyses.



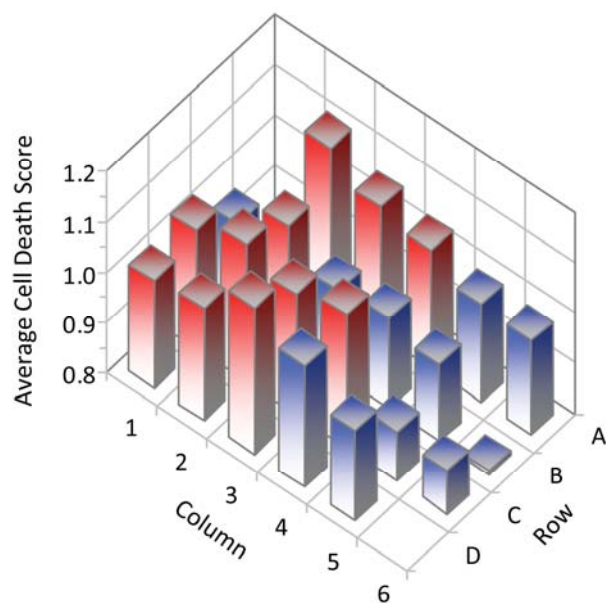
Online Figure I. Modifications to Seahorse XF24 Instrument. **A:** Top view showing fiber bundle and read head. Gas flow tubes and direction of flow are highlighted by red arrows. **B:** Front view showing gas flow lines connected to XF cartridge (green). Cut-out in aluminum side panel to permit connection at rear of plate can be seen. **C:** Placement of reflective object (razor blade) in front of instrument light sensor, to permit removal of main cover. Marker tape (orange) on support tray outside the instrument ensures correct placement of the blade prior to cover removal.



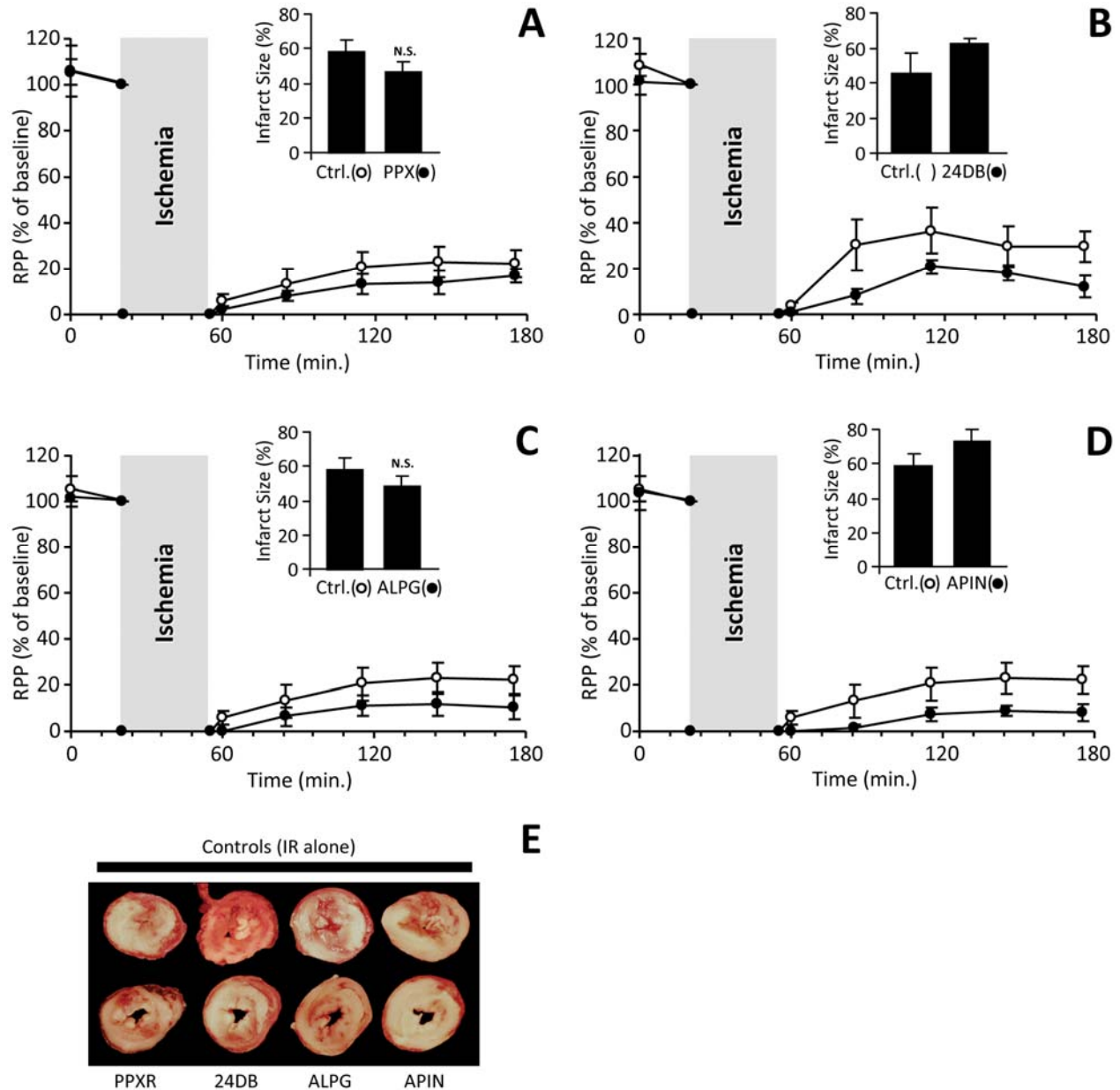
Online Figure II. Pre-validation tests, with known cardioprotective agents. Cells were subjected to IR injury as described in the methods, in the presence of the following cardioprotective agents, at the concentrations listed: adenosine (Adn, 50 μM), diazoxide (Dzx, 10μM), carbonyl cyanide 4-(trifluoromethoxy)phenylhydrazine (FCCP, 50 nM), cyclosporin A (CsA, 0.2 μM), and nitro-linoleic and nitro-oleic acids (LANO₂, OANO₂, 1 μM). Graph shows cell death, relative to controls on the same plate. Data are means ± SEM, N>9. *p<0.05 vs. control (ANOVA).



Online Figure III. Cell death data in order of assay. These data are the same as those in Fig. 3 of the main manuscript, without sorting by score. **A:** Cell death in round 1. Each point represents 1 well containing 4 test molecules ($N = 500$). **B:** Cell death in round 2. Each point represents 1 well containing 1 molecule ($N = 224$). The dotted line shows a linear regression fit, indicating an upward trend, consistent with the second round screen beginning with the most protective wells from the first round (on the left).



Online Figure IV. Map showing mean cell death in each well across all 39 plates. Protective scores (<1) are colored blue, while detrimental scores (>1) are colored red. Wells A1 and D6 were used for background control (media only), so yielded no cell death data. This average map was used to correct cell death values on individual plates, as described in the supplemental methods.



Online Figure V. Effect of detrimental and non-protective molecules identified from the screen, in IR injury in the intact heart. In addition to the 5 beneficial molecules from the screen (Table 1), 4 additional molecules were tested – propoxur (no effect), and 2,4-DB, apiin and allopregnanolone (detrimental). Molecules were administered to perfused rat hearts at 1 μ M for 20 min., prior to 35 min. ischemia and 2 hr. reperfusion. Contractile function (rate x pressure product, RPP) is expressed as % of the value immediately prior to ischemia. Data are shown for **A:** propoxur (PPX), **B:** 2,4-dichlorophenoxybutyrate (24DB), **C:** allopregnanolone (ALPG), and **D:** apiin (APIN). Following reperfusion, infarct size was determined by TTC staining, with

representative ventricular cross section images shown in panel **E**. (white = infarct, red = live tissue). Insets to panels **A-D** show infarct data for each group. Note that different controls were used for each molecule tested. All data are means \pm SEM, $N = 5-7$.

Online Table I. Full data set (cell death) for 500 test wells in round 1 and 224 test wells in round 2 are available as a Microsoft Excel™ spreadsheet.

Online Table II. List of 37 most protective molecules, ranked by score, and selection criteria for ongoing study. Chemical structures were obtained from the literature and prepared in ChemDraw software. Molecular weight (Mw, parent molecule, not salt) and LogP were calculated in ChemDraw. Other chemical properties and adherence to Lipinski's *Rule of 5*, with Ghose's filter applied⁵, were screened using Chemaxon's "chemicalize" engine (www.chemicalize.org). Disposition (column 6) refers to the decision making process behind whether to advance the molecule into perfused heart studies. Classifications are as follows:

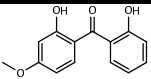
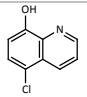
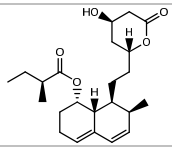
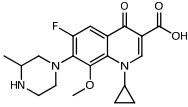
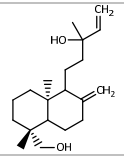
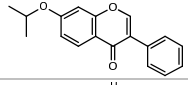
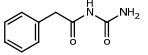
OK: Molecule satisfactory for further testing.

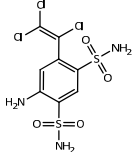
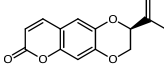
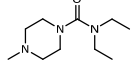
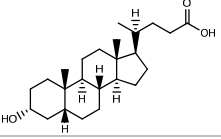
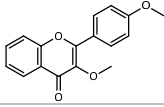
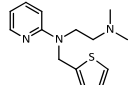
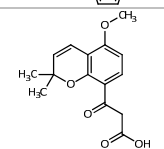
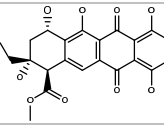
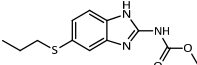
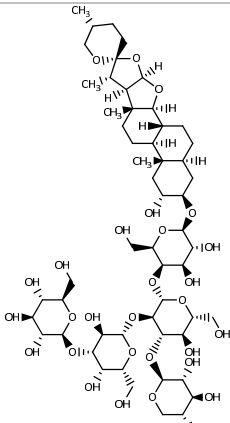
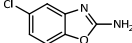
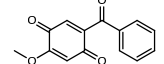
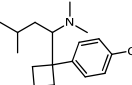
CV = Cardiovascular pharmacology or toxicity that would preclude use in CVD patients.

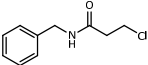
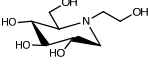
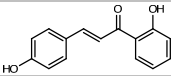
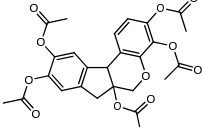
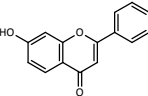
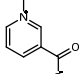
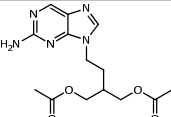
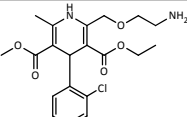
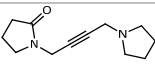
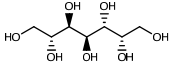
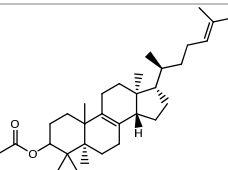
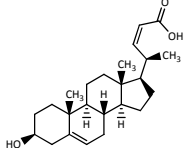
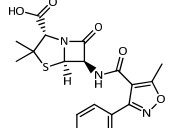
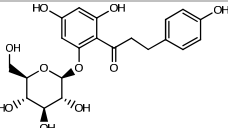
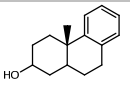
NA = Not commercially available (either at all, or in sufficient quantities for testing).

KAI = Known anti-ischemic protective properties (based on previous literature).

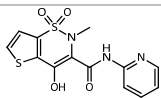
R5 = Rule of 5 incompatible, or other chemical properties sub-optimal for druggability.

Score	Compound	Structure	Mw*	LogP	Disposition	Bioactivity, Notes, References
0.546	Dioxybenzone		244.2	2.34	OK	UVA/UVB Blocker used in sun screen.
0.580	Cloxyquin		179.6	2.29	OK	Antimycobacterial. Similar to clioquinol (Chinoform), a Zn chelator which stimulates autophagy ⁶ and uncouples mitochondria ⁷ .
0.581	Mevastatin		390.5	3.35	OK KAI	Cholesterol lowering agent. Protects cardiomyocytes from IR injury via GSK-3β inhibition ⁸ .
0.621	Gatifloxacin		375.4	1.51	CV	Ocular antibiotic (Gatiflo). No effect on ACS in PROVE-IT-TIMI22 ⁹ . Raises ¹⁰ or lowers ¹¹ blood glucose. Blocks cardiac HERG channel ¹² .
0.631	Epi(13)torulosol		306.5	4.47	NA	Antibacterial from larch bark ¹³ .
0.659	Cysteamine	$H_2N-CH_2-CH_2-SH$	77.1	-0.34	KAI	Used to treat cystinuria (Cystagon). Protects cardiomyocytes vs. IR injury [17999914]
0.674	Ipriflavone		280.3	3.44	KAI	Synthetic isoflavone. Lowers cardiac O ₂ consumption ¹⁴ .
0.676	Phenacemide		146.2	1.92	OK	Anticonvulsant (Phenurone). Inhibits aldose reductase ¹⁵ .

0.687	Clorsulon		380.7	0.58	OK	Antihelminthic, used w. Ivermectin. Phosphoglycerate kinase inhibitor ¹⁶ .
0.689	Obliquin		244.2	2.18	NA	Coumarin from <i>Cedrelopsis grevei</i> (Katafray tree).
0.709	Diethyl-carbamazine		199.3	0.09	CV	Antifilarial, used w. Ivermectin. Lipoxygenase inhibitor ¹⁷ . Effects on cardiac contractility via norepinephrine release [1252670].
0.716	Lithocholic Acid		376.6	5.30	R5	Bile acid. Vitamin D receptor agonist ¹⁸ . Extends lifespan in yeast ¹⁹ .
0.721	3,4'-Dimethoxy-flavone		282.3	2.14	OK	Aryl hydrocarbon receptor antagonist ²⁰ .
0.732	Methapyrilene		261.4	3.41	OK	Antihistamine, anticholinergic, sedative.
0.733	Ursinoic acid		276.3	1.57	NA	From <i>Angelica ursina</i> (giant hogweed).
0.737	Rutilantinone		295.4	8.00	NA R5	Identified as a fatty acid uptake inhibitor by HTS ²¹ .
0.740	Albendazole		265.3	2.55	OK	Antihelminthic, used w. Ivermectin or diethylcarbamazine. Fumarate reductase inhibitor ²² .
0.748	Digitonin		1215.3		R5	Detergent.
0.751	Zoxazolamine		168.6	1.62	R5	Skeletal muscle relaxant (Flexin).
0.751	2-Benzoyl-5-methoxy benzoquinone		242.2	-0.14	NA	Synthetic analog of dalbergione, from rosewood.
0.757	Sibutramine		279.8	5.22	CV	Anorexiant (Meridia). Withdrawn due to CV risk ²³ .

0.758	Beclamide		197.7	1.83	OK	Anticonvulsant (Posedrine).
0.760	Miglitol		207.2	-2.66	KAI R5	Alpha-glucosidase inhibitor (Acarbose). Protects vs. IR (Circ. Res. 2009 120:5388-5389, Abstract #735)
0.767	2',4-Dihydroxy-chalcone		240.3	2.81	NA	From malabar nut.
0.772	Haematoxylin pentaacetate		512.5	1.37	R5	Microscopy stain.
0.778	7-Hydroxy-flavone		238.2	2.68	OK	Vasorelaxant. Possibly via K _{Ca} channels ²⁴ .
0.779	Trigonelline		137.1	N/A	NA	Niacin derivative, alkaloid found in coffee and fenugreek.
0.792	Famciclovir		321.3	-0.68	R5	Antiviral (herpes).
0.802	Amlodipine		408.9	0.29	KAI	Antianginal (Norvasc). Dihydropyridine Ca ²⁺ channel blocker. Protects vs. IR <i>in vivo</i> in dogs ²⁵ .
0.815	Oxotremorine		206.3	0.24	KAI	Muscarinic acetylcholine receptor agonist [8330013]. Prevents post-MI arrhythmias [1382385].
0.822	D-Perseitol		212.2	-3.47	R5	Structural analog of mannitol. Polyol sugar of D-mannoheptulose, a hexokinase inhibitor [5319361]
0.822	Euphol Acetate		468.8	8.40	NA R5	Triterpenoid, anti-cancer.
0.824	3βHydroxy-23,24-bisnorchole-5-enic acid		372.5	4.80	NA	Bile acid in meconium ²⁶ .
0.829	Oxacillin		401.4	2.32	CV	β-lactam antibiotic. Usage linked to cardiomyopathy [15226978]
0.834	Phloridzin		436.4	0.21	KAI	Glycosuric ²⁷ . Inhibits Na ⁺ dependent glucose transporter (SGLT, expressed in cardiomyocytes) ²⁸ . Prevents IR induced tachycardia (Circulation. 2009;120:S655. Abstract #2517)
0.834	3αHydroxy-4,4-bisnor-8,11,13-podocaratriene		216.3	3.58	NA	From Podocarpus family of trees.

0.837 Tenoxicam



337.4

0.27

KAI

NSAID, antipyretic, analgesic (Mobiflex).
(protects in neural ischemia [15756931])

	<i>Post-IR dP/dt_{MAX} recovery (%)</i>	<i>Post-IR -dP/dt_{MIN} recovery (%)</i>	<i>Ischemic Hyper- contracture (mmHg)</i>
Ctrl. Beneficial	16.1±3.9	14.8±3.0	61.3±4.3
Cloxyquin	35.4±5.4*	32.5±5.8*	36.2±5.2*
Methapyrilene	32.2±5.5*	29.4±4.6*	32.1±6.5*
Mevastatin	35.5±9.9	31.0±9.4	49.7±3.6
Clorsulon	45.8±16.2	41.6±13.9	36.9±7.4*
7-Hydroxyflavone	42.4±8.1*	34.0±6.1*	50.1±3.7
Ctrl Detrimental	24.1±6.3	21.2±4.6	39.1±5.6
Apiin	9.2±4.0*	9.0±3.9*	48.3±6.9
Propoxur	19.2±2.1	17.1±2.1	44.4±8.1
Allopregnanolone	10.7±5.3*	9.9±5.0*	48.3±6.9
2,4-DB	14.0±5.5	11.3±4.1	41.4±2.4

Online Table III. Cardiac contractility data. dP/dt_{MAX} and dP/dt_{MIN} were calculated pre- and post-IR injury from first derivatives of left ventricular pressure tracings. Data are expressed as % recovery, relative to pre-IR values. Ischemic hypercontracture refers to the end diastolic pressure at the end of ischemia, minus that 5 min. after the start of ischemia. All data are means \pm SEM, $N = 5-7$. Note that for this analysis, due to the timing of experiments beneficial molecules were studied early, and detrimental molecules later (approx' 6 months apart). Therefore, controls were expressed as two different groups – those for beneficial molecules and those for detrimental molecules, to account for temporal discrepancies in the baseline level of IR injury. * $p < 0.05$ between treatment group and control, by ANOVA.

REFERENCES

Reference List

- (1) Gerencser AA, Neilson A, Choi SW, Edman U, Yadava N, Oh RJ, Ferrick DA, Nicholls DG, Brand MD. Quantitative microplate-based respirometry with correction for oxygen diffusion. *Anal Chem* 2009;81:6868-78.
- (2) Lundholt BK, Scudder KM, Pagliaro L. A simple technique for reducing edge effect in cell-based assays. *J Biomol Screen* 2003;8:566-70.
- (3) Tompkins AJ, Burwell LS, Digerness SB, Zaragoza C, Holman WL, Brookes PS. Mitochondrial dysfunction in cardiac ischemia-reperfusion injury: ROS from complex I, without inhibition. *Biochim Biophys Acta* 2006;1762:223-31.
- (4) Nadtochiy SM, Burwell LS, Ingraham CA, Spencer CM, Friedman AE, Pinkert CA, Brookes PS. In vivo cardioprotection by S-nitroso-2-mercaptopyrionyl glycine. *J Mol Cell Cardiol* 2009;46:960-8.
- (5) Ghose AK, Viswanadhan VN, Wendoloski JJ. A knowledge-based approach in designing combinatorial or medicinal chemistry libraries for drug discovery. 1. A qualitative and quantitative characterization of known drug databases. *J Comb Chem* 1999;1:55-68.
- (6) Park MH, Lee SJ, Byun HR, Kim Y, Oh YJ, Koh JY, Hwang JJ. Clioquinol induces autophagy in cultured astrocytes and neurons by acting as a zinc ionophore. *Neurobiol Dis* 2011;42:242-51.
- (7) Yamanaka N, Imanari T, Tamura Z, Yagi K. Uncoupling of oxidative phosphorylation of rat liver mitochondria by chionoform. *J Biochem* 1973;73:993-8.
- (8) Bergmann MW, Rechner C, Freund C, Baurand A, El JA, Dietz R. Statins inhibit reoxygenation-induced cardiomyocyte apoptosis: role for glycogen synthase kinase 3beta and transcription factor beta-catenin. *J Mol Cell Cardiol* 2004;37:681-90.
- (9) Taylor-Robinson D, Boman J. The failure of antibiotics to prevent heart attacks. *BMJ* 2005;331:361-2.
- (10) Arce FC, Bhasin RS, Pasmantier R. Severe hyperglycemia during gatifloxacin therapy in patients without diabetes. *Endocr Pract* 2004;10:40-4.
- (11) Brogan SE, Cahalan MK. Gatifloxacin as a possible cause of serious postoperative hypoglycemia. *Anesth Analg* 2005;101:635-6, table.
- (12) Kang J, Wang L, Chen XL, Triggle DJ, Rampe D. Interactions of a series of fluoroquinolone antibacterial drugs with the human cardiac K⁺ channel HERG. *Mol Pharmacol* 2001;59:122-6.

- (13) Xue JJ, Fan CQ, Dong L, Yang SP, Yue JM. Novel antibacterial diterpenoids from *Larix chinensis* Beissn. *Chem Biodivers* 2004;1:1702-7.
- (14) Feuer L, Barath P, Strauss I, Kekes E. Experimental studies on the cardiological effects of ipriflavone on the isolated rabbit heart and in rat and dog. *Arzneimittelforschung* 1981;31:953-8.
- (15) Whittle SR, Turner AJ. Anti-convulsants and brain aldehyde metabolism: inhibitory characteristics of ox brain aldehyde reductase. *Biochem Pharmacol* 1981;30:1191-6.
- (16) Schulman MD, Ostlind DA, Valentino D. Mechanism of action of MK-401 against *Fasciola hepatica*: inhibition of phosphoglycerate kinase. *Mol Biochem Parasitol* 1982;5:133-45.
- (17) Lewis RA, Austen KF. The biologically active leukotrienes. Biosynthesis, metabolism, receptors, functions, and pharmacology. *J Clin Invest* 1984;73:889-97.
- (18) Ishizawa M, Matsunawa M, Adachi R, Uno S, Ikeda K, Masuno H, Shimizu M, Iwasaki K, Yamada S, Makishima M. Lithocholic acid derivatives act as selective vitamin D receptor modulators without inducing hypercalcemia. *J Lipid Res* 2008;49:763-72.
- (19) Goldberg AA, Richard VR, Kyryakov P, Bourque SD, Beach A, Burstein MT, Glebov A, Koupaki O, Boukh-Viner T, Gregg C, Juneau M, English AM, Thomas DY, Titorenko VI. Chemical genetic screen identifies lithocholic acid as an anti-aging compound that extends yeast chronological life span in a TOR-independent manner, by modulating housekeeping longevity assurance processes. *Aging (Albany NY)* 2010;2:393-414.
- (20) Lee JE, Safe S. 3',4'-dimethoxyflavone as an aryl hydrocarbon receptor antagonist in human breast cancer cells. *Toxicol Sci* 2000;58:235-42.
- (21) Li H, Black PN, Chokshi A, Sandoval-Alvarez A, Vatsyayan R, Sealls W, DiRusso CC. High-throughput screening for fatty acid uptake inhibitors in humanized yeast identifies atypical antipsychotic drugs that cause dyslipidemias. *J Lipid Res* 2008;49:230-44.
- (22) Barrowman MM, Marriner SE, Bogan JA. The fumarate reductase system as a site of anthelmintic attack in *Ascaris suum*. *Biosci Rep* 1984;4:879-83.
- (23) James WP, Caterson ID, Coutinho W, Finer N, Van Gaal LF, Maggioni AP, Torp-Pedersen C, Sharma AM, Shepherd GM, Rode RA, Renz CL. Effect of sibutramine on cardiovascular outcomes in overweight and obese subjects. *N Engl J Med* 2010;363:905-17.
- (24) Calderone V, Chericoni S, Martinelli C, Testai L, Nardi A, Morelli I, Breschi MC, Martinotti E. Vasorelaxing effects of flavonoids: investigation on the possible involvement of potassium channels. *Naunyn Schmiedebergs Arch Pharmacol* 2004;370:290-8.

- (25) Gross GJ, Farber NE, Pieper GM. Effect of amlodipine on myocardial functional and metabolic recovery following coronary occlusion and reperfusion in dogs. *Cardiovasc Drugs Ther* 1989;3:535-43.
- (26) St Pyrek J, Sterzycki R, Lester R, Adcock E. Constituents of human meconium: II. Identification of steroidal acids with 21 and 22 carbon atoms. *Lipids* 1982;17:241-9.
- (27) Ehrenkranz JR, Lewis NG, Kahn CR, Roth J. Phlorizin: a review. *Diabetes Metab Res Rev* 2005;21:31-8.
- (28) Banerjee SK, McGaffin KR, Pastor-Soler NM, Ahmad F. SGLT1 is a novel cardiac glucose transporter that is perturbed in disease states. *Cardiovasc Res* 2009;84:111-8.